ELSEVIER

Physics of the Earth and Planetary Interiors 124 (2001) 283–294

PHYSICS OF THE EARTH AND PLANETARY INTERIORS

www.elsevier.com/locate/pepi

Instability of Ekman–Hartmann boundary layers, with application to the fluid flow near the core–mantle boundary

Benoît Desjardins [a], Emmanuel Dormy [b,c,*], Emmanuel Grenier [d]

[a] *C.E.A/D.I.F., B.P. 12, 91680 Bruyères le Châtel, France*
[b] *I.P.G.P., 4 place Jussieu, 75252 Paris Cedex 05, France*
[c] *C.N.R.S., Paris, France*
[d] *U.M.P.A., E.N.S. Lyon, 46 allée d'Italie, 69364 Lyon Cedex 07, France*

Received 26 June 2000; accepted 6 October 2000

Abstract

Our aim is to investigate the instability of mixed Ekman–Hartmann boundary layers arising in rotating incompressible magnetohydrodynamics flows in a parameter regime relevant to the Earth liquid core. We perform a local study in a half space at a given co-latitude $\theta \neq \pi/2$, and assume a mean dipolar axial magnetic field with internal sources. Instabilities are driven, for high enough Reynolds number, by the quadratic term in the momentum equation. Following the work of Lilly [J. Atmos. Sci. 23 (1966) 481], we restrict our analysis to the linearized growth phase. We describe the dependence of the critical Reynolds number in terms of θ and Elsasser number (measuring the relative strength of Lorentz and Coriolis terms). It is found that no matter how large the Elsasser number is, there exists a critical band centered on the equator in which instabilities can occur. For geophysically relevant values of parameters, this band extends over some 45° away from the equator. This study establishes the possibility of boundary layer instabilities near the core–mantle boundary.

Keywords: Core–mantle boundary; Ekman–Hartmann layers; Earth core dynamics

1. Introduction

The magnetohydrodynamic flow in the Earth's core is believed to support a self excited dynamo process responsible for the Earth's magnetic field. Though one has very few means of access to the deep interior of our planet, most of the parameters characterizing the dynamics in the core are relatively well known (Poirier, 1991, 1994). One can model the Earth's core by a spherical shell, filled with a conducting fluid of density ρ, kinematic viscosity ν, conductivity σ, which rotates rapidly with angular velocity Ω. We will only consider here phenomena occurring close to the outer bounding sphere. Important parameters are the Ekman number E, the Rossby number ε, the Elsasser number Λ and the magnetic Reynolds number $\mathcal{R}_\mathrm{m}$. These are defined introducing the magnetic diffusivity $\eta = (\sigma\mu_0)^{-1}$, a typical velocity U, length scale $\mathcal{L}$ and magnetic field $\mathcal{B}$ as

$$E = \frac{\nu}{2\Omega\mathcal{L}^2}, \qquad \varepsilon = \frac{U}{2\Omega\mathcal{L}},$$
$$\Lambda = \frac{\mathcal{B}^2}{2\Omega\rho\mu_0\eta}, \qquad R_\mathrm{m} = \frac{U\mathcal{L}}{\eta}. \tag{1}$$

The role of boundary layers on the dynamics of the core and on the geodynamo is usually thought to be

* Corresponding author.
E-mail address: dormy@ipgp.jussieu.fr (E. Dormy).

0031-9201/01/$ – see front matter
PII: S0031-9201(01)00210-2

small. The laminar Ekman layer effect on the main flow, through the Ekman suction, scales as $E^{1/2}$. The Ekman suction is even reduced by magnetic effects (Acheson and Hide, 1973). This would of course be very different if the boundary layers happened to be unstable (they could then extend over a larger domain and would most probably affect the main flow). Recent studies showed that pure Ekman layer instabilities could indeed produce field generation and act as a dynamo (Ponty et al., 2000). In the last few years, numerous numerical models of self excited dynamos have been proposed (see Dormy et al. (2000) for a review). Among these models, some suppressed boundary layers using stress-free boundary conditions (Busse et al., 1999; Christensen et al., 1999; Katayama et al., 1999; Kuang and Bloxham, 1997, 1999). This was proven to strongly modify the moderate Ekman number solutions with a conducting inner core (Kuang and Bloxham, 1997; Christensen et al., 1999). Suppression of these boundary layers is based on the assumption that they are stable, and thus, small and negligible. Other numerical models retained the Ekman layers and observed a large field induction in laminar layers near the core–mantle boundary (CMB) for moderate values of the Ekman number (Sakuraba and Kono, 1999). The evidence of instabilities of these layers would shed some new light on the flow near the CMB, but also on numerical models for the dynamo.

We present a linearized study for instability of the mixed Ekman–Hartmann boundary layers in rotating incompressible magnetohydrodynamic flows. It is known (Gilman, 1971) that Ekman–Hartmann layer (as the Ekman layer and the Hartmann layer) are unstable to two-dimensional rolls for sufficiently high Reynolds numbers. The purpose of this work is to extend previous instability studies (Leibovich and Lele, 1985; Lilly, 1966; Gilman, 1971), to incompressible MHD flows near a spherical boundary at a given co-latitude $\theta \in [0, \pi/2)$ for dipolar static magnetic field. The Reynolds number at which these instabilities occur, as well as the details of these instabilities, are the subject of this article. The possibility for such instabilities to occur near the CMB will then be discussed.

2. Model description

2.1. Laminar Ekman–Hartmann boundary layer

We focus in this study to the parameter range relevant for the Earth's core, and in particular small value of the magnetic Prandtl number ($E\mathcal{R}_m\varepsilon^{-1}$). We perform a local analysis at a given co-latitude, assuming a dipolar axial mean magnetic field with internal sources. More precisely, we consider a half space $\mathcal{D}$ filed with an incompressible conducting fluid governed by the Navier–Stokes equations coupled with the induction equation

$$\begin{cases} \partial_t \boldsymbol{u} + \boldsymbol{u}\cdot\boldsymbol{\nabla}\boldsymbol{u} + \dfrac{\boldsymbol{\nabla} p}{\varepsilon} + \dfrac{\boldsymbol{e}_\Omega \times \boldsymbol{u}}{\varepsilon} - \dfrac{E}{\varepsilon}\Delta\boldsymbol{u} = \dfrac{\Lambda}{\varepsilon R_m}\operatorname{curl}\boldsymbol{B}\times\boldsymbol{B} \\ \partial_t \boldsymbol{B} = \operatorname{curl}(\boldsymbol{u}\times\boldsymbol{B}) + \dfrac{1}{\mathcal{R}_m}\Delta\boldsymbol{B}, \quad \operatorname{div}\boldsymbol{B} = 0, \qquad \operatorname{div}\boldsymbol{u} = 0 \end{cases} \tag{2}$$

where $\boldsymbol{e}_\Omega$ denotes the constant unit vector in the direction of rotation, $\boldsymbol{B}$ the magnetic field, and $\boldsymbol{E} = (\operatorname{curl}\boldsymbol{B})/\mathcal{R}_m - \boldsymbol{u}\times\boldsymbol{B}$ the electric field.

Outside the shell ($\mathcal{D}^c$), the mantle is considered to be an electrical insulator and the magnetic field is thus assumed to be harmonic

$$\operatorname{curl}\boldsymbol{B} = 0, \qquad \operatorname{curl}\boldsymbol{E} = -\partial_t\boldsymbol{B},$$
$$\operatorname{div}\boldsymbol{E} = 0, \qquad \operatorname{div}\boldsymbol{B} = 0. \tag{3}$$

At the CMB $\partial\mathcal{D}$, we require the velocity of the fluid to vanish and the tangential component of the electric field and magnetic field to be continuous.

We consider in the sequel the following orderings for ε, Λ, $\mathcal{R}_m$, E

$$\varepsilon \to 0, \quad \Lambda \sim \mathcal{O}(1), \quad \varepsilon\mathcal{R}_m \to 0, \quad E \sim \varepsilon^2. \tag{4}$$

These limits are relevant to the Earth's core (Dormy et al., 1998; Desjardins et al., 1999).

We define our frame of reference (x, y, z) with x in the $\boldsymbol{e}_1$ direction (co-latitude), y in the $\boldsymbol{e}_2$ direction (longitude) and z in the $\boldsymbol{e}_3$ direction (radial direction) (see Fig. 1).

We also assume that the direction of the static magnetic field $\boldsymbol{B}_0$ varies in latitude as a pure axial

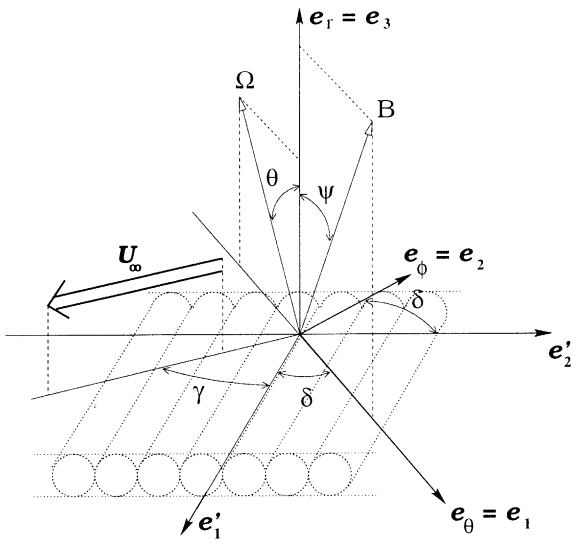

Fig. 1. Geometry of the local study. Rotation vector and magnetic field, respectively, make an angle θ and ψ with the normal to the boundary. Traveling wave solutions are sought for an external velocity $\boldsymbol{U}_\infty$. These quantities, respectively, make an angle δ and $\gamma_0 = \delta + \gamma$ with the plane ($\boldsymbol{\Omega}$, $\boldsymbol{B}$).

dipole with internal sources, so that we can write $\boldsymbol{e}_\Omega = (-\sin\theta, 0, \cos\theta)$, $\boldsymbol{e}_B = e'/||e'||$ with $e' = (\sin\theta, 0, 2\cos\theta)$ and hence

$$\cos\psi = \frac{2\cos\theta}{(1+3\cos^2\theta)^{1/2}} \quad \text{is the vertical component of } \boldsymbol{B}_0. \tag{5}$$

Note that the polarity of the field can be reversed through a modification of ψ in $\pi + \psi$, what does not affect the rest of the study.

Note also that the first assumption here is that the static magnetic field $\boldsymbol{B}_0$ has only two non-zero coordinates b_1 and b_3. If such was not the case, a second angle (say ψ_H) would need to be introduced at this stage. The dipolar variation of the field's direction (i.e. the precise relation between θ and ψ), however, becomes important only in Section 2.5 and following.

Introducing the normal Elsasser number $\Lambda_\perp = \Lambda\cos^2\psi(\cos\theta)^{-1}$, it is convenient to define τ such that $\tan\tau = \Lambda_\perp^{-1}$. With this definition, the width of the laminar Ekman–Hartmann boundary layer $\lambda\mathcal{L}$ varies (see Acheson and Hide, 1973; Desjardins et al., 1999) as

$$\lambda = \sqrt{\frac{2E\tan(\tau/2)}{\cos\theta}}, \tag{6}$$

where

$$\tan(\tau/2) = \frac{\cos\theta}{\Lambda\cos^2\psi + (\Lambda^2\cos^4\psi + \cos^2\theta)^{1/2}}. \tag{7}$$

The boundary layers are obtained by introducing the scaled vertical coordinate $z' = z/\lambda$. Assuming that the limit flow at $z' = \infty$ has the form $\boldsymbol{U}_\infty = (\cos\gamma_0, -\sin\gamma_0, 0)$ and that the magnetic field vanishes at infinity, one obtains (Acheson and Hide, 1973; Benton and Loper, 1969, 1970; Gilman and Benton, 1968; Loper, 1970a,b) a stationary velocity profile (U, V, $W = 0$) and magnetic profile (B_1, B_2, $B_3 = 0$),

$$\begin{aligned}
U(z') &= \cos\gamma_0 - \mathrm{e}^{-z'}\cos\left(z'\tan(\tau/2) + \gamma_0\right),\\
V(z') &= -\sin\gamma_0 + \mathrm{e}^{-z'}\sin\left(z'\tan(\tau/2) + \gamma_0\right),\\
B_1(z') &= -\sqrt{\frac{E\sin\tau}{\cos\theta}}\,\mathrm{e}^{-z'}\\
&\qquad \cos\left(\frac{\tau}{2} + z'\tan(\tau/2) + \gamma_0\right)\cos\psi,\\
B_2(z') &= \sqrt{\frac{E\sin\tau}{\cos\theta}}\,\mathrm{e}^{-z'}\\
&\qquad \sin\left(\frac{\tau}{2} + z'\tan(\tau/2) + \gamma_0\right)\cos\psi.
\end{aligned} \tag{8}$$

So that the velocity at infinity makes an angle $-\gamma_0$ with the x direction (i.e. $\boldsymbol{e}_\theta$).

It should be noted that Loper (1970a,b) demonstrated that this profile does not depend on the conductivity of the outer domain ($\mathcal{D}^c$). This result, however, does not extend to the following sections (instability).

2.2. Ekman–Hartrnann boundary layer instabilities

The laminar Ekman–Hartmann boundary layer profile (8) is known (Gilman, 1971) to be unstable to two-dimensional disturbances for sufficiently high Reynolds number. The relevant number here is the boundary layer Reynolds number, it is defined as the classical Reynolds number ($u\ell/\nu$), but using a typical length scale ℓ based on the boundary layer width, rather than the problem size.

For the Ekman layer at the pole, it is expressed as

$$Re_0 = \varepsilon\sqrt{\frac{2}{E}}. \tag{9}$$

If we now define the local boundary layer Reynolds number Re on the scale λ, we can write

$$Re = \frac{\lambda\varepsilon}{E}. \tag{10}$$

This quantity is constructed on the width of the Ekman–Hartmann boundary layer which varies with θ and Λ. It is, thus, the relevant physical quantity. However, it needs to be compared with the local boundary Reynolds number for the Earth (which depends on latitude). The quantity Re_0 (9) used in Desjardins et al. (1999) is scaled with respect to an arbitrary length: the width of the pure Ekman layer at the poles and can thus be compared with the same quantity for the Earth's core.

In a previous work (Desjardins et al., 1999), we derived analytically a range of Reynolds number for which nonlinear stability holds. More precisely, defining the function Ξ by

$$\Xi(k) = \sqrt{1+k^2}\int_0^{+\infty} z(|\cos(kz)| + |\sin(kz)|)\,\mathrm{e}^{-z}\,\mathrm{d}z, \tag{11}$$

it was shown that if the Reynolds number Re attached to the boundary layer satisfies

$$Re = Re_0\sqrt{\frac{\tan(\tau/2)}{\cos\theta}} < Re_s = \frac{1}{\Xi(\tan(\tau/2))}, \tag{12}$$

the corresponding MHD flow is nonlinearly stable (see Eq. (7) for the definition of $\tan(\tau/2)$ and Fig. 2). Note that $\Xi(k)$ is not defined here as in Desjardins et al. (1999), since we consider the local value of the Reynolds number Re instead of a global estimate Re_0. In our previous study, we concluded that assuming an order one Reynolds number Re_0 for the boundary layer near the CMB, stability could only be demonstrated locally near the poles if the Elsasser number was above unity. Re_s is probably a poor bound on Re. We will now study the linearized problem to establish with accuracy the boundary layer Reynolds number for instability.

Numerical simulations will yield upper bounds Re_i such that if

$$Re > Re_i(\Lambda, \theta), \tag{13}$$

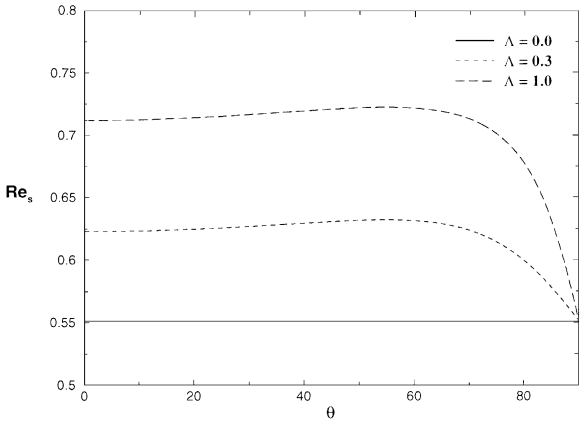

Fig. 2. Representation of an analytical result from our previous study (Re_s), here using present conventions. If the Reynolds number Re attached to the boundary layer is lower than Re_s, non-linear stability is demonstrated. We concentrate in the sequel on boundary layer Reynolds number above Re_s.

the Ekman–Hartmann flow is linearly unstable. We establish that the flow is then unstable in the following sense: there exists arbitrarily small initial perturbations which grow exponentially in time in the linear phase and reach a non negligible size (i.e. the supremum of the difference between the velocities of the perturbed flow and the unperturbed one does not go to 0 as ε goes to 0). However, we do not demonstrate mathematically that the energy of the perturbation grows significantly. The corresponding non-linear analysis is postponed to further study.

In the absence of electromagnetic coupling and for the co-latitude $\theta = 0$, Lilly (1966) showed that the pure Ekman flow is linearly unstable to two-dimensional disturbances when the boundary layer Reynolds number exceeds a critical value ($Re_i \simeq 54.16$). This study was extended to the Ekman–Hartmann profile by Gilman (1971) (still for a horizontal boundary). Leibovich and Lele (1985) extended this approach in the pure Ekman case to a spherical boundary and demonstrated the importance of the horizontal component of $\boldsymbol{\Omega}$. The case of the Ekman–Hartmann layer near a spherical boundary (in the sense $\boldsymbol{\Omega}$ and $\boldsymbol{B}_0$ vary with θ) is addressed in the present work.

A finer estimate than (4) can be achieved for geophysical parameters (Poirier, 1991, 1994; Hulot et al.,

1990). We use the radius of the core as length $\mathcal{L}$ and the following values: $||B_d|| \simeq 5 \times 10^5$ nT, $\rho \simeq 10^4\,\mathrm{kg\,m^{-3}}$, $\mu_0 \simeq 4\pi \times 10^{-7}\,\mathrm{T\,m\,A^{-1}}$, $\eta \simeq 1.1\,\mathrm{m^2\,s^{-1}}$, $\nu \simeq 10^{-6}\,\mathrm{m^2\,s^{-1}}$, $\Omega \simeq 7.3 \times 10^{-5}\,\mathrm{rad\,s^{-1}}$ and $||\boldsymbol{u}|| \simeq 10\,\mathrm{km\,per\,year} \simeq 3 \times 10^{-4}\,\mathrm{m\,s^{-1}}$.

This yields the following values for non-dimensional numbers

$$\Lambda \simeq 0.13, \quad \varepsilon \simeq 6 \times 10^{-7}, \quad E \simeq 5.5 \times 10^{-16},$$
$$\mathcal{R}_\mathrm{m} \simeq 9.5 \times 10^2, \quad Re_0 \simeq 35.6. \tag{14}$$

A few words on two important simplifications are needed. First, we will neglect large scale electrical currents (corresponding to curl $\boldsymbol{B}_0$) in their interactions with the induced field and second we only consider the dipolar component of the magnetic field (B_d) when constructing $\boldsymbol{B}_0$ and evaluating Λ.

The interaction of small scale currents curl $\boldsymbol{b}$ with large scale field $\boldsymbol{B}_0$ is of order $1/\lambda$. The interaction of large scale currents curl $\boldsymbol{B}_0$ with $\boldsymbol{b}$, however, does not enter this order. Physically, this last term is scaled as $1/L$, where L is based on magnetic diffusion. Clearly for the limits considered here (4) the ratio of viscosity to magnetic diffusivity ($\mathcal{R}_\mathrm{m} E\varepsilon^{-1}$) tends to zero and this effect can be neglected.

The toroidal component of the field can indeed be neglected here, as it needs to vanish near the insulating mantle. Writing the magnetostrophic equilibrium near the core mantle boundary would yield

$$\frac{\partial B_\mathrm{tor}}{\partial r} \sim \mu_0 \rho \frac{2\Omega u}{B_d} \simeq 4 \times 10^{-7}\,\mathrm{T\,m^{-1}}. \tag{15}$$

It is clear that B_tor would remain much smaller than B_d in the area of interest for our study (a few meters thick).

The Elsasser number thus evaluated is lower than unity and the Reynolds number Re_0 greater than 1, it is then reasonable to study precisely the onset of instability, since non-linear stability was not established in Desjardins et al. (1999) for this parameter régime.

2.3. Linearized system

Let us consider linearized perturbations ($\boldsymbol{u}$, p, $\boldsymbol{b}$) of the stationary profile (8). Magnetic perturbations are scaled according to $\boldsymbol{B} = \boldsymbol{e}_B + \mathcal{R}_\mathrm{m}\boldsymbol{b}$. Coordinates are scaled as $x' = \lambda^{-1}x, t' = \lambda^{-1}t$. Then, dropping the primes, we obtain

$$\frac{\varepsilon}{\lambda}(\partial_t \boldsymbol{u} + \boldsymbol{U}\cdot\boldsymbol{\nabla}\boldsymbol{u} + \boldsymbol{u}\cdot\boldsymbol{\nabla}\boldsymbol{U}) - \frac{E}{\lambda^2}\Delta\boldsymbol{u} + \frac{\boldsymbol{\nabla}p}{\lambda}$$
$$= \frac{\Lambda}{\lambda}\mathrm{curl}\,\boldsymbol{b}\times\boldsymbol{e}_B - \boldsymbol{e}_\Omega\times\boldsymbol{u}$$
$$+\frac{\Lambda\mathcal{R}_\mathrm{m}}{\lambda}(\mathrm{curl}\,\boldsymbol{B}\times\boldsymbol{b} + \mathrm{curl}\,\boldsymbol{b}\times\boldsymbol{B}), \quad \mathrm{div}\,\boldsymbol{u} = 0, \tag{16}$$

$$\frac{R_\mathrm{m}}{\lambda}(\partial_t\boldsymbol{b} + \boldsymbol{U}\cdot\boldsymbol{\nabla}\boldsymbol{b} + \boldsymbol{u}\cdot\boldsymbol{\nabla}\boldsymbol{B} - \boldsymbol{b}\cdot\boldsymbol{\nabla}\boldsymbol{U} - \boldsymbol{B}\boldsymbol{\nabla}\boldsymbol{u})$$
$$= \frac{1}{\lambda}\mathrm{curl}(\boldsymbol{u}\times\boldsymbol{e}_B) + \frac{1}{\lambda^2}\Delta\boldsymbol{b}, \quad \mathrm{div}\,\boldsymbol{b} = 0. \tag{17}$$

We will consider perturbations which are plane traveling waves (see Fig. 1) and we will change the reference frame (x, y, z) to (x', y', z) such that x' derivatives of $(\boldsymbol{u}, p, \boldsymbol{b})$ vanish. We, therefore, introduce the angle δ between the intersection of the plane of the waves and the plane (x, y) and the projection of e and e' on the plane (x, y).

We then rotate coordinates (x, y) by an angle δ to get (x', y'). In the sequel, the primes of x' and y' are dropped. In this new frame, $(\boldsymbol{u}, p, \boldsymbol{b})$ are independent of x, and

$$\boldsymbol{e}_\Omega = (-\sin\theta\cos\delta,\ -\sin\theta\sin\delta,\ \cos\theta),$$

$$\boldsymbol{e}_B = (\sin\psi\cos\delta, \sin\psi\sin\delta, \cos\psi).$$

We use the velocity components u along $\boldsymbol{e}_1'$, the field component b_1 along the same axis scaled as $\tilde{\beta} = b_1/(\lambda\cos\psi)$ and stream function $\tilde{\phi}$ with vector potential $\tilde{\mathcal{X}}$ in the normal plane.

We now take traveling wave type perturbations $\tilde{\phi}$, $\tilde{\mathcal{X}}$, u and $\tilde{\beta}$ as follows:

$$\tilde{\phi}(t, y, z) = \phi(z)\,\mathrm{e}^{i\alpha(y-ct)},$$
$$\tilde{\mathcal{X}}(t, y, z) = \mathcal{X}(z)\,\mathrm{e}^{i\alpha(y-ct)},$$
$$u(t, y, z) = \mu(z)\,\mathrm{e}^{i\alpha(y-ct)},$$
$$\tilde{\beta}(t, y, z) = \beta(z)\,\mathrm{e}^{i\alpha(y-ct)}. \tag{18}$$

The set of differential equations governing these perturbations (demonstration is given in the Appendix A)

can be written as

$$
\begin{aligned}
&ci\alpha\, Re(\phi'' - \alpha^2\phi) \\
&\quad = -(\phi'''' - 2\alpha^2\phi'' + \alpha^4\phi) \\
&\qquad +2\tan\frac{\tau}{2}(-\mu' + i\alpha\tan\theta\sin\delta\,\mu) \\
&\qquad +i\alpha V\, Re(\phi'' - \alpha^2\phi) - i\alpha\, Re\, V''\phi \\
&\qquad -\left(1 - \tan^2\frac{\tau}{2}\right)(\mathcal{X}'''' - \alpha^2\mathcal{X}' \\
&\qquad +i\alpha\tan\psi\sin\delta\,(\mathcal{X}'' - \alpha^2\mathcal{X})),
\end{aligned}
\tag{19}
$$

$$
\begin{aligned}
&ci\alpha\, Re\,\mu \\
&\quad = -(\mu'' - \alpha^2\mu) \\
&\qquad +2\tan\frac{\tau}{2}(\phi' - i\alpha\tan\theta\sin\delta\,\phi) \\
&\qquad +i\alpha\, Re(V\mu + U'\phi) \\
&\qquad -\left(1 - \tan^2\frac{\tau}{2}\right)(\beta' + i\alpha\tan\psi\sin\delta\,\beta),
\end{aligned}
\tag{20}
$$

$$
i\alpha\tan\psi\sin\delta\mu + \mu' + \beta'' - \alpha^2\beta = 0, \tag{21}
$$

$$
\begin{aligned}
&i\alpha\tan\psi\sin\delta(\phi'' - \alpha^2\phi) \\
&\quad +\phi''' - \alpha^2\phi' + \mathcal{X}'''' - 2\alpha^2\mathcal{X}'' + \alpha^4\mathcal{X} = 0.
\end{aligned}
\tag{22}
$$

The coefficients U and V vary with z, what makes numerical computations necessary. They also depend on γ_0, minimization over γ_0 is, thus, required to get the most unstable configuration.

2.4. Boundary conditions

The system of differential equations expressed above requires 12 boundary conditions. We first state that velocity vanishes at $z = 0$, so that

$$
\phi = 0, \qquad \phi' = 0, \qquad \mu = 0 \text{ at } z = 0.
$$

Moreover, we assume that the tangential component of the electric field and the magnetic field are continuous across the interface (Roberts, 1967b). In the insulator, we can use the x invariance to write the magnetic field $\boldsymbol{b}$ in terms of $\tilde{\beta}$ and vector potential $\tilde{\mathcal{X}}$, as in Section 2.3, which leads to

$$
\begin{aligned}
&\Delta_{y,z}\tilde{\mathcal{X}} = 0, \qquad \partial_z\tilde{\beta} = \partial_y\tilde{\beta} = 0, \\
&\partial_z E_1 = \mathcal{R}_m\partial_t\partial_z\tilde{\mathcal{X}}, \qquad \partial_y E_1 = \mathcal{R}_m\partial_t\partial_y\tilde{\mathcal{X}}.
\end{aligned}
$$

Hence, taking $\boldsymbol{E}$ and $\boldsymbol{b}$ in the insulator as in (18), we deduce

$$
E_1 = -i\alpha c\mathcal{R}_m\mathcal{X}, \text{ and } \mathcal{X}'' - \alpha^2\mathcal{X} = 0.
$$

In particular, $\mathcal{X}'(0^-) = \alpha\mathcal{X}(0^-)$, and the continuity of E_1 across the interface reduces to

$$
\mathcal{X}''(0^+) = \alpha\mathcal{X}(0)(\alpha - ic\mathcal{R}_m).
$$

At infinity, we assume, as in Lilly (1966), that $\partial_z u$, $\partial_z v$, w, and $\partial_z^2 b_1$, $\partial_z^2 b_2$, $\partial_z b_3$ vanish, and write

$$
\begin{aligned}
&\phi = 0, \quad \phi'' = 0, \quad \mu' = 0, \text{ and } \beta'' = 0, \\
&\mathcal{X}' = 0, \quad \mathcal{X}''' = 0 \text{ at infinity.}
\end{aligned}
$$

Thus, the 12 conditions needed are expressed.

2.5. Relevant equilibria

As stressed in Leibovich and Lele (1985), in the pure Ekman case ($\Lambda = 0$), the θ and δ dependence of system (19–22) only relies on the parameter

$$
\xi = \tan\theta\sin\delta.
$$

First, it is useful to note that this parameter vanishes in the horizontal plane case. This highlights that though the laminar layer only depends on the normal component of $\boldsymbol{\Omega}$, the instabilities are affected by its horizontal component as well (Leibovich and Lele, 1985). The parameter ξ accounts for this effect.

It should be noted that changing δ into $\pi - \delta$ does not modify ξ, and thus does not affect the Reynolds number. This implies that if $\delta \neq \pi/2$, two instabilities with angles δ and $\pi - \delta$ occur for the same critical Reynolds number.

The minimizing value ξ^* of ξ is obtained in Leibovich and Lele (1985). For $\xi = \xi^*$, the boundary layer Reynolds number for instability (Re_i) is minimal. At low values of θ, $\xi = \xi^*$ cannot be realized and $\delta = \pi/2$ is required to have large values of ξ, as close as possible to ξ^*. Past a critical co-latitude $\theta^* = \text{atan}(\xi^*) \simeq 63.8^\circ$, the value of ξ, and thus, the Reynolds number for instability, can be maintained constant ($\xi = \xi^*$) through a proper variation of the angle δ

$$
\delta = \delta_1 = \text{asin}\left(\frac{\xi^*}{\tan\theta}\right),
$$

or

$$
\delta = \pi - \delta_1.
$$

Near the equator, as $\tan\theta$ increases, δ_1 tends to zero, and the rolls get aligned with $\boldsymbol{e}_1$ (north–south).

In the mixed Ekman–Hartmann régime ($\Lambda \neq 0$), relevant to the Earth core, for an arbitrary imposed magnetic field, a similar reasoning leads to introducing

$$\xi' = \tan\psi \sin\delta.$$

The boundary layer Reynolds number for instability is then a function of both ξ and ξ', and the two parameters describe the full θ, ψ, δ dependence. Note that both ξ and ξ' vanish for $\theta = \psi = 0$. The terms, respectively, reflect the role of the horizontal component of $\boldsymbol{\Omega}$ and $\boldsymbol{B}_0$ on the instabilities.

If the imposed field varies in latitude as an axial dipole, ψ and θ are related through (5), so that constant values for ξ and ξ' cannot be maintained through a simple variation of δ, and thus, the critical Reynolds number will not be constant at low latitudes once $\Lambda \neq 0$. Note that neither ξ nor ξ' is affected by a, modification of θ in $\pi + \theta$, however, the profiles (8) are modified and we arbitrarily chose to restrict, our study to one hemisphere: $\theta \in [0, \pi/2]$.

Note also that neither ξ nor ξ' is affected by a modification of δ in $\pi - \delta$. This modification, therefore, leaves the Reynolds number unaffected, as was the case previously in the non-magnetic régime (both angles are unstable for the same boundary layer Reynolds number).

Because we assumed a perfectly dipolar variation of the static magnetic field (Eq. (5)), the value $\theta = \pi/2$ is singular both for the Ekman layer Greenspan (1969) and the Hartmann layer (Roberts, 1967a). As the value of θ increases toward the equator, the stable mixed Ekman–Hartmann boundary layer, however, degenerates to an Ekman layer. Indeed for $(\pi/2 - \theta) < \Lambda^{-1}$ rotation dominates. As a consequence, the equatorial singularity relevant to our study is the Ekman layer singularity. It scales as $E^{1/5}$ in the axial direction and as $E^{2/5}$ in the radial direction (e.g. Kleeorin et al., 1997). Our study is limited by the size of this singularity (which we do not intend to describe here), and thus, to values of θ smaller than $\pi/2 - E^{1/5}$. For geophysically realistic values of E, a thin strip of width 10^{-3} rad near the equator is to be excluded.

The instability Eqs. (19)–(22) in the magnetic régime ($\Lambda \neq 0$) still differ from the simple Ekman equations (i.e. $\Lambda = 0$) near the equator, because of the term associated with the horizontal component of the imposed magnetic field. But, as in the non-magnetic régime, δ must tend to zero (in order to maintain ξ and ξ' finite), also for the field we consider $\tan(\tau/2)$ tends to unity. As a consequence, all magnetic effects vanish near the equator, and the instability itself evolves toward the pure Ekman layer instability. Physically, this is related to the invariance of the pure Ekman layer instability with respect to the direction $\boldsymbol{e}_1$, the horizontal component of the imposed magnetic field lies precisely along this direction near the equator ($\delta = 0$) and does not affect the instability.

3. Numerical results

3.1. Validation

We developed a Fortran-90 code to compute the critical Reynolds number Re above which instabilities appear, resolving Eqs. (19)–(22). Eigenvalues of complex matrices were computed using the EISPACK library from Netlib (http://netlib.bell-labs.com/netlib/eispack). The gradient algorithm was parallelized using the MPI library. Results were tested successfully against previous studies: in the non-magnetic régime (Leibovich and Lele, 1985; Lilly, 1966), as well as in a horizontal plane in the pure Hartmann limit (Roberts, 1967b) and in the mixed Ekman–Hartmann régime (Gilman, 1971).

3.2. Results

We find that the layer is linearly unstable if $Re_0 > Re_i(\Lambda, \theta)$. We represent in Fig. 3 the critical Reynolds number Re_i versus the co-latitude θ, for different values of the Elsasser number $\Lambda \in \{0, 0.3, 1\}$. One can note on this figure that the critical Reynolds number for instability is no longer independent of θ at low latitudes once $\Lambda \neq 0$ as expected from the discussion in Section 2.5.

We can then construct an approximate estimate for the local boundary layer Reynolds number at the CMB

$$Re_{\mathrm{BL}} = \varepsilon \sqrt{\frac{2}{E}} \sqrt{\frac{\tan(\tau/2)}{\cos\theta}}. \tag{23}$$

Note, however, that this estimate is proportional to the estimation on ε, and thus, $\|\boldsymbol{u}\|$. The estimation (14) is based on secular variation studies (Bloxham and Jackson, 1992; Hulot et al., 1990) and represent a

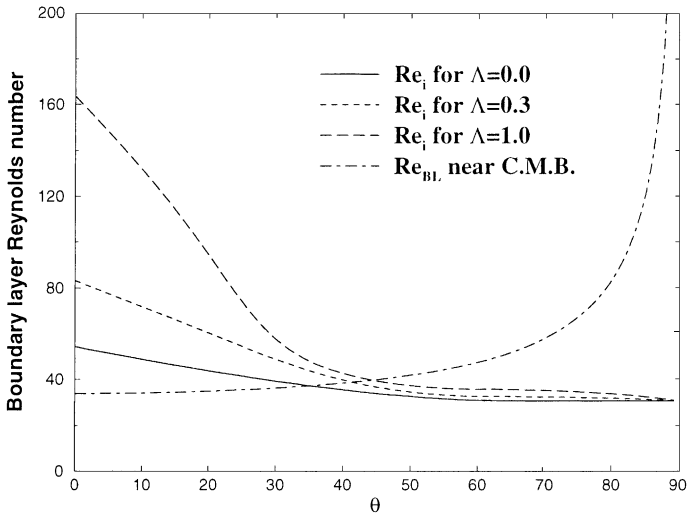

Fig. 3. Boundary layer Reynolds number for instability for three different values of the Elsasser number vs. co-latitude θ. An estimation of the boundary layer Reynolds number near the core–mantle boundary is also represented for comparison.

typical velocity near the CMB. It is clear, however, that the velocity could locally be at least twice as large and could also be several order smaller at other places; the value of Re_{BL} would then undergo the same variations. It is, thus, important to consider Re_{BL} as an estimate only. Re_{BL} computed from (14) and (23) is also represented on Fig. 3.

For the parameter range (14) relevant to the Earth core, there exists a critical co-latitude θ_{c} below which the Ekman–Hartmann boundary layer can be linearly unstable. From the estimated Re_{BL}, one would get $\theta_{\mathrm{c}} \simeq 45^{\circ}$.

We would like to stress that, we previously established in Desjardins et al. (1999) the value below which non-linear stability could be proven (Re_s). This value being estimated analytically, it probably represents a poor estimate. However, comparing this value (see Fig. 2) with the present results (Re_i), a coefficient close to 50 is obtained for $\Lambda = 0.3$. This much lower value of Re_s could suggest, a possible subcritical bifurcation of the Ekman–Hartmann layer.

Let us now describe physically the instability (for $Re = Re_i$). The angle δ at which the instability grows is represented versus co-latitude θ on Fig. 4. The instability is aligned with the $\boldsymbol{e}_\phi$, direction near the pole for the three Elsasser numbers considered here. Past a critical co-latitude two branches of solution exist, corresponding to δ and $\pi - \delta$, as described in Section 2.5. This critical value of the co-latitude (noted θ^* in the non-magnetic case) decreases with Λ, as the horizontal component of the imposed magnetic field lies in the $\boldsymbol{e}_\theta$ direction and magnetic effects reduce shear in this direction (maximum when $\delta = 90^{\circ}$). Near the equator, the instability is aligned with $\boldsymbol{e}_\theta$ in the magnetic régime as in the $\Lambda = 0$ case.

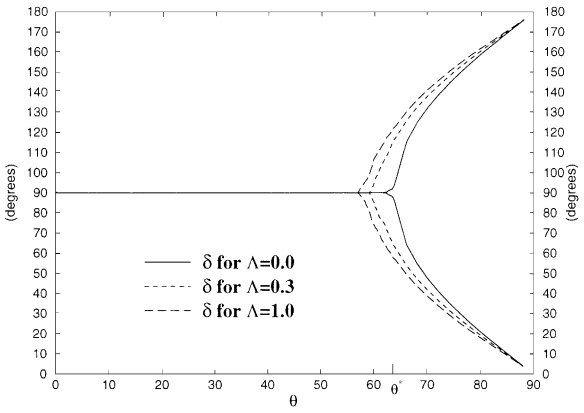

Fig. 4. Angles δ for instability with respect to $\boldsymbol{e}_\theta$ represented vs. the co-latitude θ. The instability develops in the $\boldsymbol{e}_\phi$ direction near the poles. Past a critical co-latitude (decreasing with Λ) two branches of solutions exist. The instability is aligned with $\boldsymbol{e}_\theta$ near the equator.

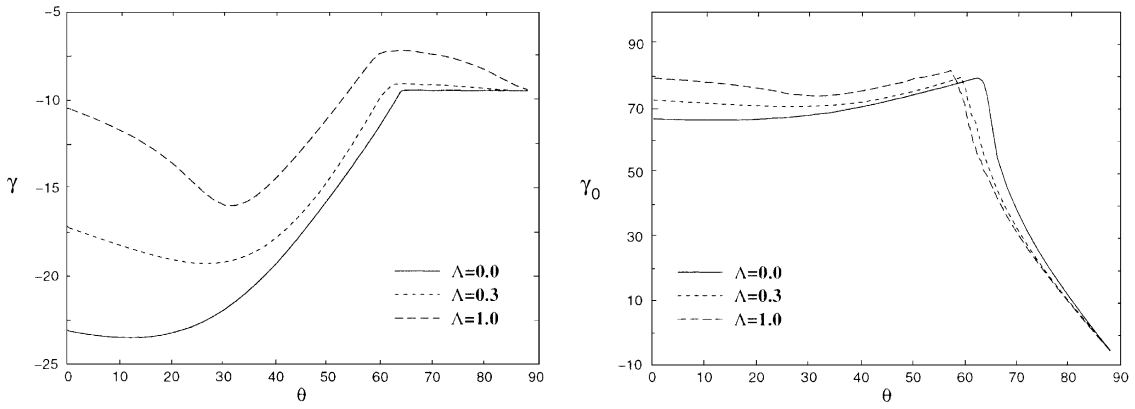

Fig. 5. Angles γ on the left and $\gamma_0 = \delta + \gamma$ (between the $\boldsymbol{e}_\theta$ direction and $\boldsymbol{U}_\infty$) on the right, both represented vs. co-latitude θ.

Angles γ between $\boldsymbol{e}_1'$ and the $\boldsymbol{U}_\infty$ flow corresponding to these instabilities (which enters Eqs. (19)–(22) through the expressions of U and V) are represented in Fig. 5, together with $\gamma_0 = \delta + \gamma$ corresponding to the angle between the $\boldsymbol{e}_\theta$ direction and $\boldsymbol{U}_\infty$ (see also Fig. 1, for angles construction).

The wave number α and the corresponding phase velocity $\alpha \times c_r$ are represented on Fig. 6. The solution propagates in the azimuthal direction in the equatorial region and towards the poles away from the equator.

3.3. Geophysical discussion

When trying to develop an intuitive understanding of the stability of the boundary layer near the Earth's CMB (an Ekman–Hartmann type of boundary layer), one can hesitate between two main lines of thinking. The first one states that the Reynolds number in the core is so high (around 10^8) that, one can hardly imagine anything laminar in the flow. The other lines that the layer is so thin ($\mathcal{L}E^{1/2}$ would represent less than a meter) that instabilities are unlikely to develop there. Probably the first geophysically relevant result of our work is to show how these two effects compensate and how the boundary layer near the core mantle boundary is extremely close to instability.

For geophysically realistic values of the control parameters, a critical band is found to extend over some 45° away from the equator (see Fig. 3). It is, however, useful to recall that Re_{BL} is only an estimate based on

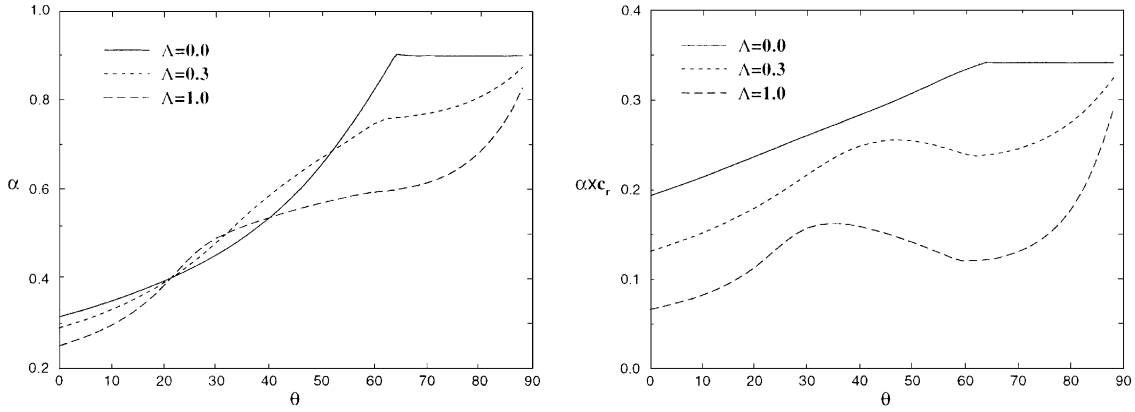

Fig. 6. Wave number α on the left and the corresponding phase velocity $\alpha \times c_r$ on the right, both represented vs. co-latitude θ.

a typical value of $\|\boldsymbol{u}\|$ and that its value is, therefore indicative.

The critical value for instability being so close to geophysical estimates, it appears useful to discuss with additional care the limitations of our study. We computed here the minimal Reynolds number after minimizing on γ (measuring the direction of $\boldsymbol{U}_\infty$). This direction could, in the Earth, be far from optimum. For example, an optimal Re_i, was obtained near the equator for $\gamma_0 = \delta + \gamma \simeq -10^\circ$ whereas in the Earth, flows near the CMB inferred from variations of the magnetic field (Bloxham and Jackson, 1992) are rather found to be aligned in the longitudinal direction near the equator ($\gamma_0 = \delta + \gamma \simeq \pm 90^\circ$). Also, we assumed a perfectly spherical boundary. This, however, seems reasonable as bumps at the CMB are known to be small about 4 km for wavelength larger than 300 km (Garcia and Sourian, 2000) and they would only slightly modify the results. We assumed that the static field varies in latitude as a perfect dipole, this certainly is not the case in the Earth. In particular, as the geographic equator and the magnetic equator would differ almost everywhere the normal component of the field may stabilize the flow near the geographic equator. This effect is, however, expected to be small. We assumed a perfectly insulating mantle. This is a reasonable assumption, as conductivity of the lower mantle is known to be very small (Alexandrescu et al., 1999) and the existence of a thin conductive layer appears most unlikely (Poirier et al., 1998). There are also some physical effects, not included in our model, that could alter the critical boundary layer Reynolds number. In particular effects of density perturbations were neglected. Buoyancy effects could modify the stability of the layer (see Braginsky (1999) for geophysical discussion of density profile near the CMB). Thermal effects could also possibly be associated with current sheets near the insulating mantle, this could help destabilize the layer. Also we insist again that, when comparing results with the estimated boundary Reynolds number near the CMB (Re_{BL}), only an order of magnitude was used for a $\|\boldsymbol{u}\|$. The problem of possible boundary layer instabilities near the CMB clearly deserves further study (especially concerning more complicated large scale fields and the effects of the direction of $\boldsymbol{U}_\infty$ and of the non dipolar component of the field), such study could rely on field map at the CMB and core flows derived from the secular variation of the field. This could also allow to test a possible relation between boundary layer instabilities and rapid geomagnetic impulses (or jerks) observed some eight times in the last century (Alexandrescu et al., 1995, 1996; Courtillot and Le Mouël, 1984; Mac Millan, 1996).

Acknowledgements

We acknowledge extremely useful discussions with Jean-Louis Le Mouël, that helped significantly to improve the manuscript. Authors have also benefited from fruitful discussions with Yann Brenier, Dominique Jault and Gauthier Hulot. E.D. is very grateful to Professor Andrew Soward for enlightening discussions about boundary layers and their singularities. The authors wish to remind that any error in this work would be their responsibility only. Numerical computations were performed on the Alphaservers' Cluster at the D.M.P.N. of Institute de Physique du Globe de Paris.

Appendix A. Mathematical construction of instability equations

Let us first recall that we have assumed in (4) that

$$\varepsilon \to 0, \quad \Lambda \sim \mathcal{O}(1), \quad \varepsilon \mathcal{R}_{\mathrm{m}} \to 0, \quad E \sim \varepsilon^2.$$

and that the magnetic field $\boldsymbol{B}$ was expended as $\boldsymbol{B} = \boldsymbol{e}_B + \mathcal{R}_{\mathrm{m}} \boldsymbol{b}$.

We consider perturbations of the stationary profile (8). However, B_1 and B_2 being of order $E^{1/2}$, only $\boldsymbol{e}_B$ is relevant here.

As $\boldsymbol{b}$ is of order ε, we can rewrite (16)–(17) as

$$Re\left(\partial_t \boldsymbol{u} + V\partial_y \boldsymbol{u} + w\frac{\mathrm{d}U}{\mathrm{d}z}\right) + \frac{\lambda^2}{E}\begin{vmatrix} -v\cos\theta - w\sin\theta\sin\delta \\ u\cos + w\sin\theta\cos\delta \\ -v\sin\theta\cos\delta + u\sin\theta\sin\delta \end{vmatrix} + \frac{\lambda}{E}\begin{vmatrix} 0 \\ \partial_y p - \Delta_{y,z}\boldsymbol{u} \\ \partial_{\boldsymbol{z}} p \end{vmatrix} = \frac{\Lambda\lambda}{E}\begin{vmatrix} \partial_z b_1 \cos\psi + \partial_y b_1 \sin\psi\sin\delta \\ -\partial_y b_1 \sin\psi\cos\delta - j_1\cos\psi \\ -\partial_z b_1 \sin\psi\cos\delta + j_1 \sin\psi\sin\delta \end{vmatrix} \quad (A.1)$$

where $j_1 = \partial_y b_3 - \partial_z b_2$, and

$$\lambda(\sin\psi\sin\delta\,\partial_y \boldsymbol{u} + \cos\psi\,\partial_z \boldsymbol{u}) + \Delta_{y,z}\boldsymbol{b} = 0 \quad (A.2)$$

We will now use the velocity and field components along the axis of instability; in the normal plane, the divergence free condition on $\boldsymbol{u}$ and $\boldsymbol{b}$ yield the existence of a stream function $\tilde{\phi}$ and a vector potential $\tilde{\mathcal{X}}$ such that

$$v = -\partial_z\tilde{\phi}, \qquad w = \partial_y\tilde{\phi},$$
$$b_2 = -\lambda\cos\psi\,\partial_z\tilde{\mathcal{X}}, \qquad b_3 = \lambda\cos\psi\,\partial_y\tilde{\mathcal{X}}.$$

Denoting $\tilde{\beta} = b_1/(\lambda\cos\psi)$, $\tilde{\zeta} = \Delta_{y,z}\tilde{\phi}$ and $\tilde{\eta} = \Delta_{y,z,}\tilde{\mathcal{X}}$ and taking the first component of the curl of Eqs. (A.1) and (A.2), we deduce

$$Re(D_t\tilde{\zeta} + V\partial_y\tilde{\zeta} - V''\partial_y\tilde{\phi}) + \frac{\lambda^2}{E}(-\cos\theta\,\partial_z u + \sin\theta\sin\delta\,\partial_y u) - \Delta_{y,z}\tilde{\zeta} = \frac{\lambda^2\Lambda\cos\psi}{E}(\cos\psi\,\partial_z\tilde{\eta} + \sin\psi\sin\delta\,\partial_y\tilde{\eta}), \quad (A.3)$$

$$Re(\partial_t u + V\partial_y u + U'\partial_y\tilde{\phi}) + \frac{\lambda^2}{E}(\cos\theta\,\partial_z\tilde{\phi} - \sin\theta\sin\delta\,\partial_y\tilde{\phi}) - \Delta_{y,z}u = \frac{\lambda^2\Lambda\cos\psi}{E}(\cos\psi\,\partial_z\tilde{\beta} + \sin\psi\sin\delta\,\partial_y\tilde{\beta}), \quad (A.4)$$

$$\sin\psi\sin\delta\,\partial_y u + \cos\psi\,\partial_z u + \cos\psi\Delta_{y,z}\tilde{\beta} = 0, \quad (A.5)$$

$$\sin\psi\sin\delta\,\partial_y\tilde{\zeta} + \cos\psi\,\partial_z\tilde{\zeta} + \cos\psi\,\Delta_{y,z}\tilde{\eta} = 0. \quad (A.6)$$

We now take traveling wave type perturbations $\tilde{\phi}$, $\tilde{\mathcal{X}}$, u and $\tilde{\beta}$ as follows:

$$\tilde{\phi}(t,y,z) = \phi(z)\,e^{i\alpha(y-ct)},$$
$$\tilde{\mathcal{X}}(t,y,z) = \mathcal{X}(z)\,e^{i\alpha(y-ct)},$$
$$u(t,y,z) = \mu(z)\,e^{i\alpha(y-ct)},$$
$$\tilde{\beta}(t,y,z) = \beta(z)\,e^{i\alpha(y-ct)}, \quad (A.7)$$

and obtain an eigenvalue problem expressed in terms of a system of four ordinary differential equations:

$$ci\alpha\,Re(\phi'' - \alpha^2\phi) = -(\phi'''' - 2\alpha^2\phi'' + \alpha^4\phi) + \frac{\lambda^2}{E}(-\cos\theta\,\mu' + i\alpha\sin\theta\sin\delta\mu) + i\alpha V\,Re(\phi'' - \alpha^2\phi) - i\alpha\,Re\,V''\phi - \frac{\Lambda\lambda^2\cos\psi}{E}(\cos\psi(\mathcal{X}''' - \alpha^2\mathcal{X}') + i\alpha\sin\psi\sin\delta(\mathcal{X}'' - \alpha^2\mathcal{X})) \quad (A.8)$$

$$ci\alpha\,Re\,\mu = -(\mu'' - \alpha^2\mu) + \frac{\lambda^2}{E}(\cos\theta\,\phi' - i\alpha\sin\theta\sin\delta\,\phi) + i\alpha\,Re(V\mu + U'\phi) - \frac{\Lambda\lambda^2\cos\psi}{E}(\cos\psi\,\beta' + i\alpha\sin\psi\sin\delta\,\beta), \quad (A.9)$$

$$i\alpha\sin\psi\sin\delta\,\mu + \cos\psi\,\mu' + \cos\psi(\beta'' - \alpha^2\beta) = 0, \quad (A.10)$$

$$i\alpha\sin\psi\sin\delta(\phi'' - \alpha^2\phi) + \cos\psi(\phi''' - \alpha^2\phi') + \cos\psi(\chi'''' - 2\alpha^2\chi'' + \alpha^4\chi) = 0 \quad (A.11)$$

where the expressions $V = V(z)$, $V'' = V''(z)$, $U' = U'(z)$ in the reference frame (e_1', e_2', e_3') are obtained replacing γ_0 by $\gamma = \gamma_0 - \delta$ in (8).

Using the expression $\tan\tau = \cos\theta(\Lambda\cos^2\psi)^{-1} = \Lambda_\perp^{-1}$, the system (A.8)–(A.11) can be rewritten as

$$ci\alpha\,Re(\phi'' - \alpha^2\phi) = -(\phi'''' - 2\alpha^2\phi'' + \alpha^4\phi) + 2\tan\frac{\tau}{2}(-\mu' + i\alpha\tan\theta\sin\delta\,\mu) + i\alpha V\,Re(\phi'' - \alpha^2\phi) - i\alpha\,Re\,V''\phi - \left(1 - \tan^2\frac{\tau}{2}\right)(\mathcal{X}''' - \alpha^2\mathcal{X}' + i\alpha\tan\psi\sin\delta\,(\mathcal{X}'' - \alpha^2\mathcal{X})) \quad (A.12)$$

$$ci\alpha\,Re\,\mu = -(\mu'' - \alpha^2\mu) + 2\tan\frac{\tau}{2}(\phi' - i\alpha\tan\theta\sin\delta\,\phi) + i\alpha\,Re(V\mu + U'\phi) - \left(1 - \tan^2\frac{\tau}{2}\right) \times(\beta' + i\alpha\tan\psi\sin\delta\,\beta) \quad (A.13)$$

$$i\alpha \tan\psi \sin\delta\mu + \mu' + \beta'' - \alpha^2\beta = 0, \tag{A.14}$$

$$i\alpha \tan\psi \sin\delta(\phi'' - \alpha^2\phi) + \phi''' - \alpha^2\phi' + \mathcal{X}'''' - 2\alpha^2\mathcal{X}'' + \alpha^4\mathcal{X} = 0 \tag{A.15}$$

References

Acheson, D.J., Hide, R., 1973. Hydromagnetics of rotating fluids. Rep. Prog. Phys. 36, 159–221.

Alexandrescu, M., Gibert, D., Hulot, G., Le Mouël, J.-L., Saracco, G., 1995. Detection of geomagnetic jerks using wavelet analysis. J. Geophys. Res. 100 (B7), 12557–12572.

Alexandrescu, M., Gibert, D., Hulot, G., Le Mouël, J.-L., Saracco, G., 1996. Worldwide wavelet analysis of geomagnetic jerks. J. Geophys. Res. 101 (B10), 21975–21994.

Alexandrescu, M., Gibert, D., Le Mouël, J.-L., Hulot, G., Saracco, G., 1999. An estimate of average lower mantle conductivity by wavelet analysis of geomagnetic jerks. J. Geophys. Res. 104 (B8), 17735–17745.

Benton, E., Loper, D., 1969. On the spin-up of an electrically conducting fluid, Part 1. J. Fluid Mech. 39 (3), 561–586.

Benton, E., Loper, D., 1970. On the spin-up of an electrically conducting fluid, Part 2. J. Fluid Mech. 43 (4), 785–799.

Bloxham, J., Jackson, A., 1992. Time-dependent mapping of the magnetic field at the core–mantle boundary. J. Geophys. Res. 97, 19536–19563.

Braginsky, S.I., 1999. Dynamics of the stably stratified ocean at the top of the core. Phys. Earth Planet. Interiors 11 (1/2), 21–34.

Busse, F., Grote, E., Tilgner, A., 1999. On convection driven dynamos in rotating spherical shells. Studia Geophys. Geodyn. 42, 211–223.

Christensen, U., Olson, P., Glatzmaier, G., 1999. Numerical modelling of the geodynamo: a systematic parameter study. Geophys. J. Interiors 138, 393–409.

Courtillot, V., Le Mouël, J.-L., 1984. Geomagnetic secular variation impulses. Nature 311, 709–716.

Desjardins, B., Dormy, E., Grenier, E., 1999. Stability of mixed Ekman–Hartmann boundary layers. Nonlinearity 12, 181–199.

Dormy, E., Cardin, P., Jault, D., 1998. MHD flow in a slightly differentially rotating spherical shell, with conducting inner core, in a dipolar magnetic field. Earth Planet. Sci. Lett. 160, 15–30.

Dormy, E., Valet, J.-P., Courtillot, V., 2000. Numerical models of the Geodynamo and observational constraints. Geochem.-Geophys.-Geosyst. 1, 62.

Garcia, R., Souriau, A., 2000. Amplitude of the core–mantle boundary topography estimated by stochastic analysis of core phases. Phys. Earth and Planet. Interiors 117 (1/4), 345–359.

Gilman, P., Benton, E., 1968. Influence of an axial magnetic field on the steady linear Ekman boundary layer. Phys. Fluids 11, 2397–2401.

Gilman, P., 1971. Instabilities of the Ekman–Hartmann boundary layer. Phys. Fluids 14, 7–12.

Greenspan, H.P., 1969. The Theory of Rotating Fluids. Cambridge Monographs on Mechanics and Applied Mathematics, Cambridge.

Hulot, G., Le Mouël, J.-L., Jault, D., 1990. The flow at the core–mantle boundary: symmetry properties. J. Geomagn. Geoelectr. 42, 857–974.

Katayama, J., Matsushima, M., Honkura, Y., 1999. Some characteristics of magnetic field behavior in a model of MHD dynamo thermally driven in a rotating spherical shell. Phys. Earth Planet. Interiors 111, 141–159.

Kleeorin, N., Rogachevskii, I., Ruzmaikin, A., Soward, A.M., Starchenko, S., 1997. Axisymmetric flow between differentially rotating spheres in a dipole magnetic field. J. Fluid Mech. 344, 213–244.

Kuang, W., Bloxham, J., 1997. An Earth-like numerical dynamo model. Nature 389, 371–374.

Kuang, W., Bloxham, J., 1999. Numerical modeling of magnetohydrodynamic convection in a rapidly rotating spherical shell: weak and strong field dynamo action. J. Comput. Phys. 153, 51–81.

Leibovich, S., Lele, S.K., 1985. The influence of the horizontal component of the Earth's angular velocity on the instability of the Ekman layer. J. Fluid Mech. 150, 41–87.

Lilly, D.K., 1966. On the instability of the Ekman boundary layer. J. Atmos. Sci. 23, 481–494.

Loper, D., 1970a. General solution for the linearized Ekman–Hartmann layer on a spherical boundary. Phys. Fluids 13, 2995–2998.

Loper, D., 1970b. Steady hydromagnetic boundary layer near a rotating, electrically conducting plate. Phys. Fluids 13, 2999–3002.

Mac Millan, S., 1996. A geomagnetic jerk for the early 1990's. Earth Planet. Sci. Lett. 137, 189–192.

Poirier, J.-P., 1991. Introduction to the Physics of the Earth's Interior. Cambridge University Press, Cambridge.

Poirier, J.-P., 1994. Physical properties of the Earth's core. C. R. Acad. Sci. Paris 318, 341–350.

Poirier, J.-P., Malavergue, V., Le Mouël, J.-L., 1998. Is there a thin electrically conducting layer at the base of the mantle? In: The Core–Mantle Boundary Region, Vol. 28. AGU Geodynamics, pp. 131–137.

Ponty, Y., Gilbert, A.D., Soward, A.M., 2000. Kinematic dynamo action in flows driven by shear and convection. J. Fluid Mech., submitted for publication.

Roberts, P.H., 1967a. Singularity of Hartmann layers. Proc. R. Soc. A 300, 94–107.

Roberts, P.H., 1967b. An Introduction to Magnetohydrodynamics. Elsevier, Amsterdam.

Sakuraba, A., Kono, M., 1999. Effect of the inner core on the numerical solution of the magnetohydrodynamic dynamo. Phys. Earth Planet. Interiors 111, 105–121.